IEEE Access
Multidisciplinary | Rapid Review | Open Access Journal

SPECIAL SECTION ON GIGAPIXEL PANORAMIC VIDEO WITH VIRTUAL REALITY

Received May 16, 2020, accepted June 2, 2020, date of publication June 11, 2020, date of current version June 26, 2020.

Digital Object Identifier 10.1109/ACCESS.2020.3001128

An Improved LWD Azimuth Gamma Imaging Model Based on HSI Space

HE ZHANG[1], HONGQIANG LI[1], DENGYUN LU[2], AND YI XIE[2]
[1]School of Mechatronic Engineering, Southwest Petroleum University, Chengdu 610500, China
[2]Chuanqing Drilling Engineering Technology Research Institute, Guanghan 618300, China

Corresponding author: He Zhang (zhanghe@swpu.edu.cn)

This work was supported by the Sichuan Science and Technology Innovation and Venture Seedling Project, China, under Grant 20MZGC0139.

ABSTRACT In recent years, in the process of oil and gas exploration and development, the situation of drilling tools drilling out of the reservoir often occurs. Due to the lack of directional indication, the traditional LWD(Logging While Drilling) natural gamma measurement technology cannot guide drilling tools to return to the reservoir efficiently. In order to solve this problem, this paper improves the traditional radiometric gamma measurement technology and establishes a set of azimuth gamma imaging model. Firstly, the basic imaging model is established based on HSI (Hue, Saturation, Intensity) color space. Then, the study focuses on the design of the gamma data quality control algorithm, which can effectively suppress the original gamma data noise. In addition, the cubic spline interpolation algorithm is selected to support the model to obtain 360° omni-directional gamma data. Finally, the image processing technology based on fast grayscale grouping is applied in this study, which greatly improves the imaging effect. Field application shows that the model runs stably on site, and the azimuth gamma image is well indicative. It can monitor the relative position relationship between the borehole trajectory and the formation, which effectively improves the reservoir encounter rate, and has high application and promotion value.

INDEX TERMS Azimuth gamma imaging, HSI color space, quality control algorithm, image processing, fast grayscale grouping.

I. INTRODUCTION

In recent years, the complexity of exploration and development of oil and gas fields has gradually increased, and the formations encountered have been complicated and diverse, such as thinner and thinner formations, curved formations, and even faults [1]. Geosteering technology has become one of the necessary means for the exploration and development of oil and gas wells with these complex well conditions [2], [3]. It can more conveniently assist engineers to judge whether the drilling tool is drilling into the reservoir according to the predetermined borehole trajectory [4] in the layer. In addition, intelligent algorithm is also widely used in drilling risk assessment system [5].

The traditional LWD natural gamma [6] measures the average gamma of the formation, which does not contain azimuth information, and cannot effectively determine the structural information of the layer where the drilling tool is located. Because of the limitations of natural gamma measurement, engineers in the oil and gas exploration industry at home and abroad have improved the traditional natural gamma measurement technology to different degrees, including azimuth gamma measurement technology [7]–[9]. The measurement principle is essentially the same, but azimuth gamma is a vector data, which can not only measure the previous average gamma value of the formation, but also measure the changes of gamma at different angles around the well. Functionally, it can not only assist engineers to perform formation comparison and lithology analysis like natural gamma, but also analyze the borehole trajectory and the relative position of formations based on azimuth gamma images. However, due to the influence of complex downhole working conditions and data transmission, the azimuth gamma data measured while drilling often contain strong noise, resulting in fuzzy gamma imaging and low quality, which cannot accurately reflect the actual situation of the formation.

To solve this problem, an improved LWD azimuth gamma imaging model based on HSI color space is proposed in

The associate editor coordinating the review of this manuscript and approving it for publication was Zhihan Lv.

this paper. Firstly, the model completes imaging chromatographic design and chromaticity calibration under HSI color space; Then, this study focused on improving the azimuth gamma data sampling model, and designed a gamma data quality control algorithm to improve data quality from the source; In addition, the model optimizes the data interpolation algorithm to support 360° gamma data at any sector angle and depth interval. The azimuth gamma image generated based on the data after secondary processing is enhanced by the image processing technology based on the fast grayscale grouping, which improves the image quality, enables it to guide the field engineer to adjust the drilling trajectory of the drilling tool more clearly, and obtains better geosteering interpretation [10].

The rest of the paper is organized as follows: the second part introduces the related work. The third part elaborates the establishment of azimuth gamma imaging model based on HSI color space. The fourth part designs the improved azimuth gamma data sampling model and the gamma image enhancement method, then the simulation is carried out to verify the validity of the model. The fifth part is the field application and analysis. The sixth part is the conclusion.

II. RELATED WORK

A. RADIOACTIVE GAMMA LOGGING

Gamma ray is a stream of gamma photons that accompanies other decays. It has the smallest ionization ability and the strongest penetration ability, making it easy to be detected in oil wells with complicated ground conditions. The energy of other types of photons is generally less than 110KeV. Due to the weak energy, it is easily absorbed on the surface of the formation and tools, while the energy of gamma photons is much larger than other types of photons, generally 0.4MeV $\sim$ 5.2MeV, so It can be roughly considered that other types of photon flow have no effect on the underground gamma detector, but only consider the radioactive influence of gamma photons, so radioactive gamma logging is generally used [11].

B. LWD AZIMUTH GAMMA INSTRUMENTS

At present, near-bit measuring instrument [12] has been widely used in well logging. As shown in Figure 1, it is a near-bit tracing azimuth gamma sensor. It differs from natural gamma in that the probe azimuth gamma adds a shielding layer to the outer layer of the sensor and opens an opening in a specified direction, as shown in Figure 2, so that the formation gamma rays captured by the sensor have directionality. As the instrument rotates, the sensor can detect gamma rays in all directions, and the measured gamma ray intensity can be matched to different sectors with the help of downhole sector measurement system and directional sensor [13].

As shown in Figure 3, the geosteering data acquisition system collects real-time measurement data to the server for storage and transmission [14] through the azimuth gamma probe, winch sensor, gyro inclinometer [15], etc. The following study in this paper will be based on the original azimuth

FIGURE 1. Probe azimuth gamma sensor.

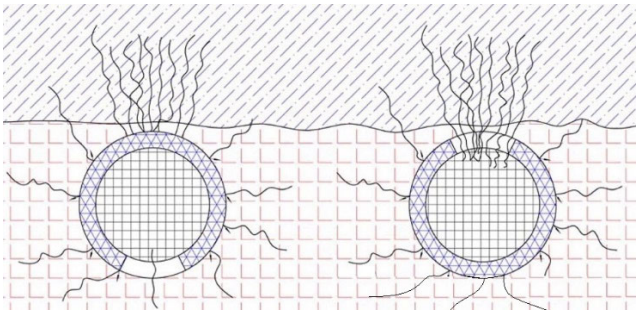

FIGURE 2. The working diagram of azimuth gamma.

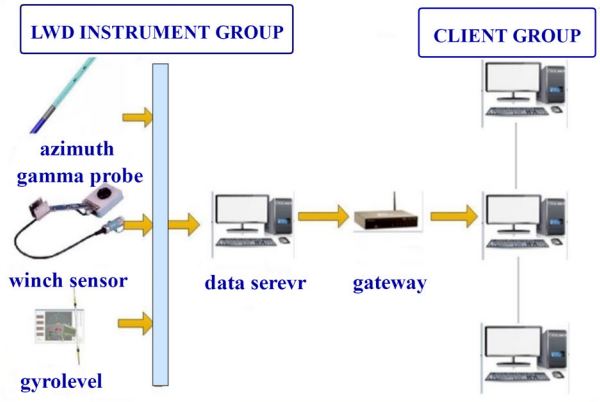

FIGURE 3. Framework diagram of geosteering data acquisition system.

gamma data collected by the system, through a series of steps of data preprocessing, data quality control, data interpolation, chromatographic design, chromaticity calibration, etc. to generate azimuth gamma images. Then, the image processing technology based on fast grayscale grouping will be used to further enhance the image quality.

C. THE RELATIONSHIP BETWEEN IMAGING INTERPRETATION AND GEOSTEERING

With the gamma imaging function, firstly, it can analyze the relative position relationship between drilling tools and

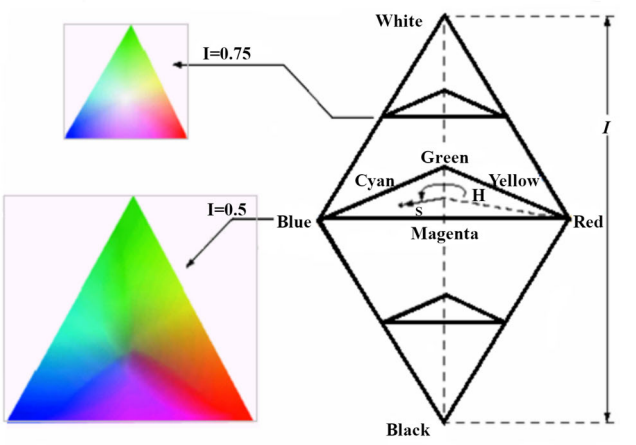

FIGURE 4. HSI color space model.

formation directly and quickly, and interpret the trajectory effectively. The ground engineer can quickly make response measures according to the imaging map, and can quickly adjust the drilling tools when they are separated from the reservoir. Secondly, when the drilling trajectory reaches the boundary of a certain formation, the change boundary line is measured directly on the imaging map, and the apparent formation dip angle of this formation is calculated in a specific way. In this way, the analysis speed is improved, and the calculation result is more accurate. In adition, the accurate angle of drilling tools back to the reservoir can be found quickly, so as to avoid the secondary out of the reservoir due to the error of angle judgment, and ensure the accurate rate of drilling tools in the oil and gas reservoir.

III. RESEARCH AND ESTABLISHMENT OF IMAGING MODEL

A. HSI COLOR SPACE

At present, most color image processing algorithms are based on RGB color space [16], in which the three components of Red (R), Green (G), and Blue (B) have a strong correlation. When the ratio of the three components changes, the image will have color distortion. The HSI color space uses Hue (H), Saturation (S) and Intensity (I) to describe color images, which is compatible with the human visual system [17]. The HSI color space model is shown in Figure 4.

Hue (H) is related to the wavelength of the light wave. It represents how the human senses feel different colors. Its value corresponds to the angle between the vector pointing to the point and the R axis. Saturation (S) indicates the purity of the color. The saturation in the center of the triangle is the smallest, and the higher the outer saturation. Intensity (I) corresponds to the imaging brightness and image grayscale, and is the brightness of the color. The HSI color space model can only consider the I component when processing color images, and does not change the color type of the image [18]. In order to suit the visual characteristics of people, reflect the formation characteristics more clearly and facilitate the observation and decision-making of drilling engineers. In this study, HSI color space is used to describe colors. Since most images are currently stored in the computer in RGB color space mode, the conversion relationship between HSI space model and RGB space model can be expressed as follows:

$$H = \begin{cases} \theta, & G \geq B \\ \pi + \theta, & G < B, \end{cases} \quad \theta = \frac{\pi}{2} - \tan^{-1}\left(\frac{2R - G - B}{\sqrt{3}\,(G - B)}\right) \tag{1}$$

$$S = \frac{2}{\sqrt{6}} \times \sqrt{(R - G)^2 + (R - B)\,(G - B)} \tag{2}$$

$$I = \frac{R + G + B}{\sqrt{3}} \tag{3}$$

where, H, S and I represent Hue, Saturation and Intensity respectively, R, G, and B represent Red, Green and Blue respectively, they are normalized to the interval [0,1] before calculation.

B. CHROMATOGRAPHIC DESIGN

In order to make the gamma images more realistically reflect the natural characteristics of the formation, low gamma values are usually represented in light colors and high gamma values in dark colors. In this study, 5 primary colors (white, yellow, orange, brown and black) were selected from light to dark, and 64 levels of chromatography were set between each adjacent primary color. According to the transformation relation described in section A(HSI color space), the chromatographic band obtained is shown in Figure 5.

C. CHROMATICITY CALIBRATION

Chromaticity calibration [19] refers to the process of measuring data that needs to be characterized as a color image, forming a certain mapping relationship between the data and color values, and then generating an image according to the mapping relationship.

Firstly, the original azimuth gamma data of the imaging well section is extracted and processed by an improved data sampling model (to be elaborated in section IV). Then the processed data is mapped from the maximum value to the minimum value according to the chromatographic band designed in section B(Chromatographic design), which can ensure that the color depth characteristics of the azimuth gamma image of the imaging well section are consistent with the characteristics of the gamma measurement value. The specific steps are as follows:

Step 1: Extract the original gamma data, and obtain the maximum value γ_{max} and minimum value γ_{min} by secondary processing.

Step 2: Correlate the γ_{max} and γ_{min} obtained in step 1 with the maximum value C_{max} and minimum value C_{min} of the chromatographic band, then calculate the chromatographic scale factor K and color scale value V_{min}, as follows:

$$K = \frac{C_{max} - C_{min}}{\gamma_{max} - \gamma_{min}} \tag{4}$$

$$V_{min} = C_{min} - \gamma_{min} \cdot K \tag{5}$$

FIGURE 5. Azimuth gamma imaging chromatographic band.

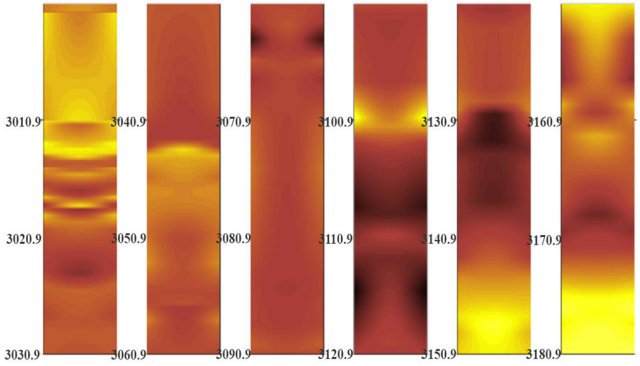

FIGURE 6. Chromaticity calibration image of a well section.

Step 3: Map the gamma value to the color scale value, as follows:

$$V_{pixel} = \gamma_i \cdot K + V_{\min} \tag{6}$$

where, V_{pixel} is the mapped color scale value; γ_i is the corresponding gamma value; K is the scale factor; and $V_{\min}$ is the color scale value corresponding to $\gamma_{\min}$. The gamma image of a certain interval calibrated according to the above steps is shown in Figure 6.

IV. ESTABLISHMENT OF IMPROVED DATA SAMPLING MODEL AND IMAGE PROCESSING

A. GAMMA DATA QUALITY CONTROL ALGORITHM

The location of formation changes during drilling is marked with depth. The drilling data used to characterize the formation changes belong to depth sequence data. Due to the influence of formation properties and measurement environment, the depth sequence can be imagined as a combination of trend and noise. Trend is the real expression of drilling measurement parameters to the formation changes, the sequence of data shows the trend changes, while the noise is the distortion of data caused by system error or environmental impact, and the amplitude of the sequence data is affected by noise. Due to the influence of the cuttings movement and the complex downhole environment, there is a lot of noise in the gamma data while drilling. In order to eliminate the influence of the original data noise without losing the original data trend characteristics, this study designed a weighted average gamma data quality control algorithm. The specific steps are as follows:

Step 1:Select the input sequence data source (x, y) and number it with (x_i, y_i), $i = 1, 2, 3, \ldots, n$;

Step 2:Take x_t as the center to intercept a section of data with length of N, and use a weighted average for this section

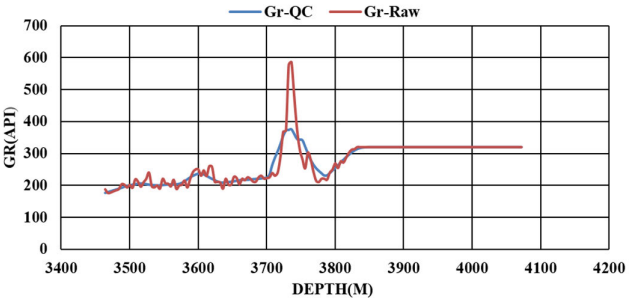

FIGURE 7. Effect comparison before and after quality control.

of data, as follows:

$$f(\hat{x}_t) = \frac{\sum_{i=t-N}^{i=t+N} K_\lambda(x_t, x_i) y_i}{\sum_{i=t-N}^{i=t+N} K_\lambda(x_t, x_i)} \tag{7}$$

Step 3:Calculate the weighted core value, as follows:

$$K_\lambda(x_t, x_i) = D\left(\frac{|x_t - x_i|}{\lambda}\right) \tag{8}$$

$$D(\mu) = \begin{cases} \frac{3}{4}(1-\mu^2) & |\mu| < 1 \\ 0 & |\mu| \geq 1 \end{cases} \tag{9}$$

$$\lambda = |x_t - x_{[k]}| \tag{10}$$

where, λ is the parameter of the weighted kernel, only considering the influence of the nearest k points, and $x_{[k]}$ is the point closest to the kth point of x_t.

Step 4: Replace the original x_t with $\hat{x}_t$, and repeat the above steps for all N data points.

The study in this paper selected the drilling data of standard formation profile in a certain oil area as the research object, as shown in Figure 7, which shows the trend characteristics and the comparison of the original data after the gamma data is processed by the quality control algorithm. In figure 7, Gr-Raw represents the original data curve, and Gr-QC represents the curve processed by the quality control algorithm. It can be seen that compared with the original data, the processed data noise is effectively controlled, while retaining the original trend characteristics of data changes, which solves the problem of system error or environmental impact in gamma data measurement. Only in this way can we effectively and comprehensively extract stratum features.

B. DATA INTERPOLATION

Limited by the downhole data transmission rate, the number of azimuth gamma values actually collected is limited, it is necessary to process from the limited number of gamma data points obtained, so that it can truly reflect the full range of formation conditions downhole. In this study, data interpolation technology is used to interpolate the scattered gamma values at different depth points. A group of gamma data measured at each depth point (taking eight sectors as an example) is interpolated as a data interval to obtain the continuous azimuth gamma curve around the well.

As shown in Table 1, the azimuth gamma data records of 8-sectors of a well section were extracted from the formation gamma ray intensity values (unit: API) of 8 directions, including 0°, 45°, 90°, 135°, 180°, 225°, 270°, 315° and 360°. In this study, linear interpolation [20], Newton interpolation [21] and cubic spline interpolation [22], [23] were used to interpolate the azimuth gamma data in eight sectors to describe the change of 360° gamma value around the well. The results are shown in Figure 8.

It can be seen from Figure 8 that the error between cubic spline interpolation and Newton interpolation is less than linear interpolation, and cubic spline interpolation has the best curve smoothness. At the same time, cubic spline interpolation is easier to evaluate than higher-order polynomials, and will not be affected by the Runge phenomenon [24]. Moreover, it can ensure that the interpolation data and derivatives are continuous, so that each interpolation point has a good correlation. Therefore, the study in this paper uses cubic spline interpolation to construct 360° gamma data around the well to ensure better continuity of raw gamma data and high smoothness of the gamma image.

C. IMAGE PROCESSING

In order to obtain more formation features from the azimuth gamma image, it is not only necessary to mark the chromaticity of the positional gamma image, but also to further process the image before the introduction of image interpretation, focusing on details, so as to enhance the image quality and improve the display effect. Image enhancement is an important means to acquire image information and improve the ability to identify information. Due to its characteristics of eliminating interference and improving image quality, image enhancement plays a crucial role in digital image processing. It has been widely used in multiple fields involving medical treatment, education, agriculture, electronics and industry [25]–[27]. Nowadays, information technology and petroleum exploration technology are developing rapidly and highly integrated, so it is more and more important to adopt image processing technology to improve logging quality in the field of logging technology.

In this study, an image enhancement algorithm based on fast grayscale grouping [28] is adopted for image processing to improve image display effect, which can ensure image interface detection and angle calculation [29].

The main idea of fast grayscale grouping is: the grayscale histogram of the original image is first created, then align it with a relatively small number of grayscale and merge it into a group, then convert it to gray level according to the creation of the enhancement function (the principle is that the pixel step size is the largest), and repeat the above process until it becomes 2 groups. The specific flow of the algorithm are as follows:

Step 1: Count the number of pixels on the K-th grayscale of the original image, and record it as $M_n(k)$.

Step 2: Grayscale grouping:

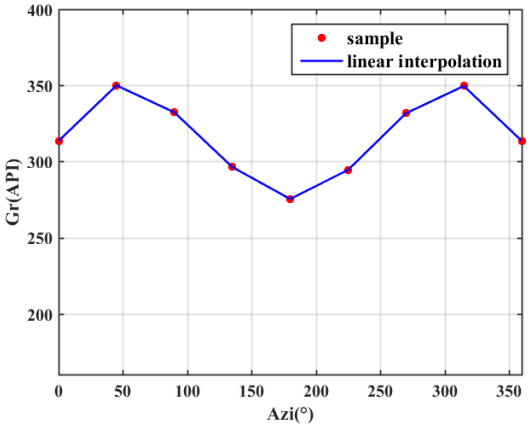

(a) Linear interpolation

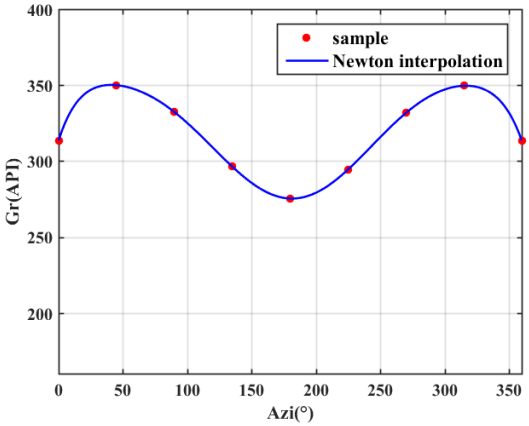

(b) Newton interpolation

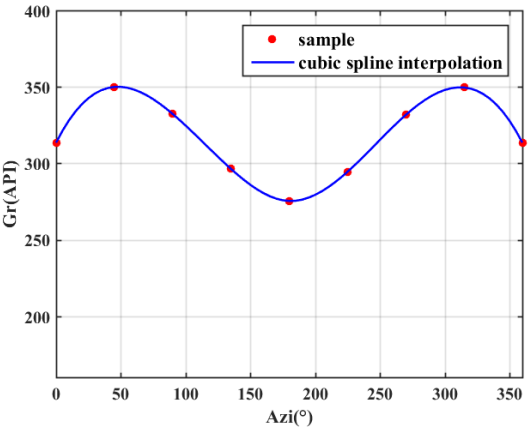

(c) Cubic spline interpolation

FIGURE 8. Comparison of different interpolation methods.

Define $P_n(i)$ as the number of pixels after grouping, and initialize it as follows:

$$P_n(i) = M_n(k) \tag{11}$$

where, $M_n(k) \neq 0, k = 0, 1, 2, \ldots m-1, i = 0, 1, 2, \ldots n$.

Define $L_n(i)$ and $R_n(i)$ are the intervals of gray levels around $P_n(i)$, and initialize it as follows:

$$L_n(i) = k, R_n(i) = k \tag{12}$$

TABLE 1. 8-sectors azimuth gamma data(part).

Depth (m)	*0°*	*45°*	*90°*	*135°*	*180°*	*225°*	*270°*	*315°*	*360°*
3001.0	313.533	349.964	332.269	296.334	275.332	294.432	331.657	349.576	313.533
3001.1	313.026	349.423	331.541	295.873	274.503	293.592	329.949	348.017	313.026
3001.2	312.521	348.563	330.815	295.015	273.675	292.971	329.242	347.053	312.521
3001.3	312.014	347.986	330.086	294.764	272.846	291.986	328.534	346.679	312.014
3001.4	311.509	347.024	329.360	296.983	272.019	291.021	327.828	345.271	311.509
3001.5	311.002	346.537	328.631	295.047	271.190	290.878	327.120	344.895	311.002

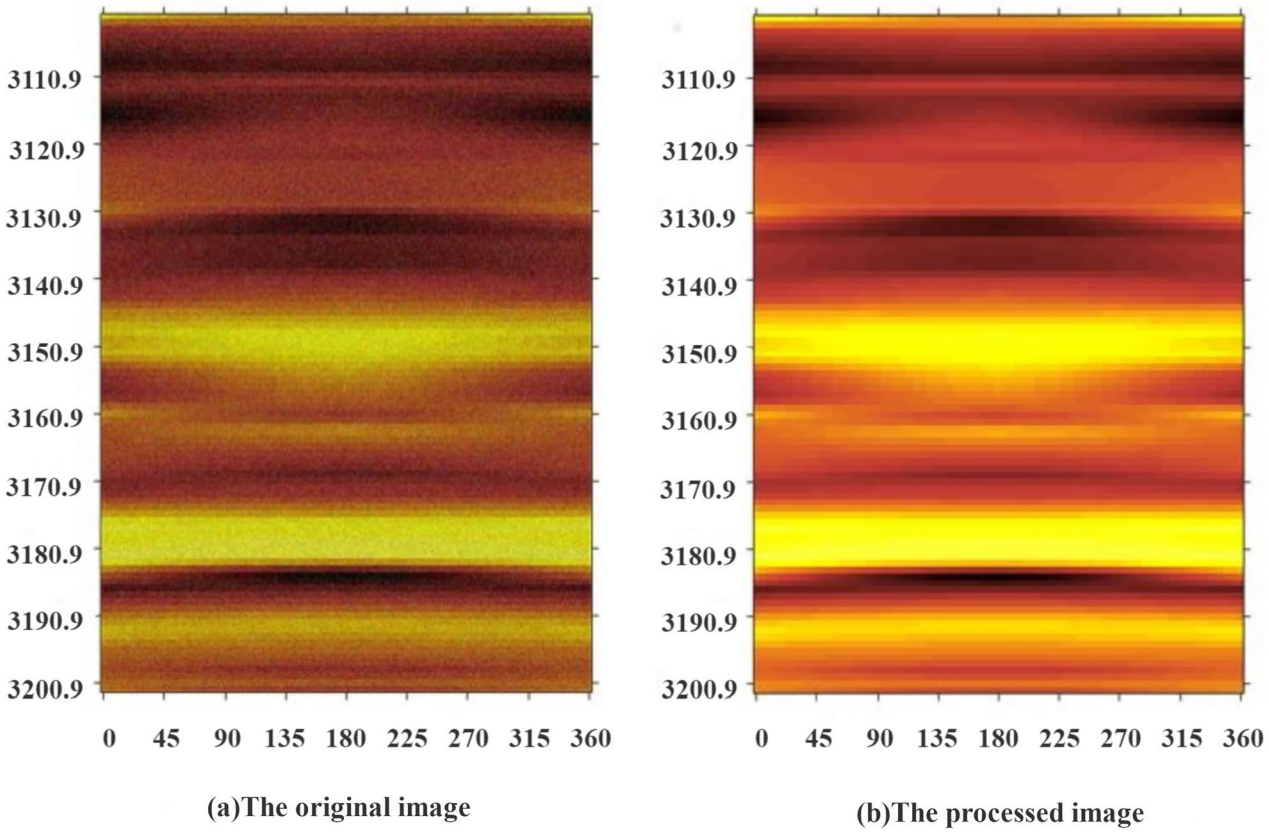

FIGURE 9. Contrast of imaging effect.

Determine the minimum value a of $P_n(i)$, and then merge it with the next smallest value to get a new group $P_{n-1}(i)$, it is expressed as follows:

$$P_{n-1}(i) = \begin{cases} P_n(i) & i = 1, 2, \ldots, j \\ a + b & i = j \\ P_{n-1}(i) & i = j+1, j+2, \ldots n+1 \end{cases} \tag{13}$$

where, $a = \min\{P_n(i)\}, b = \min\{P_n(i_a - 1), P_n(i_a + 1)\}$, $M_n(i_a) = a, j$ is expressed as follows:

$$j = \begin{cases} i_a - 1 & P_n(i_a - 1) \leq P_n(i_a + 1) \\ i_a & other \end{cases} \tag{14}$$

Step 3: Calculate the enhancement function $F_{n-1}(k)$:

1) If the grayscale k falls in $P_{n-1}(i)$, and $L_{n-1}(i) \neq R_{n-1}(i)$, $F_{n-1}(k)$ can be expressed as follows:

$$F_{n-1}(k) = \begin{cases} (i - \alpha - \dfrac{R_{n-1}(i) - k}{R_{n-1}(i) - L_{n-1}(i)})N_{n-1} + 1 \\ L_{n-1}(i) = R_{n-1}(i) \\ (i - \dfrac{R_{n-1}(i) - k}{R_{n-1}(i) - L_{n-1}(i)})N_{n-1} + 1 \\ L_{n-1}(i) \neq R_{n-1}(i) \end{cases} \tag{15}$$

2) If the grayscale k falls in $P_{n-1}(i)$ and $P_{n-1}(i+1)$, or $L_{n-1}(i) = R_{n-1}(i)$, $F_{n-1}(k)$ can be expressed

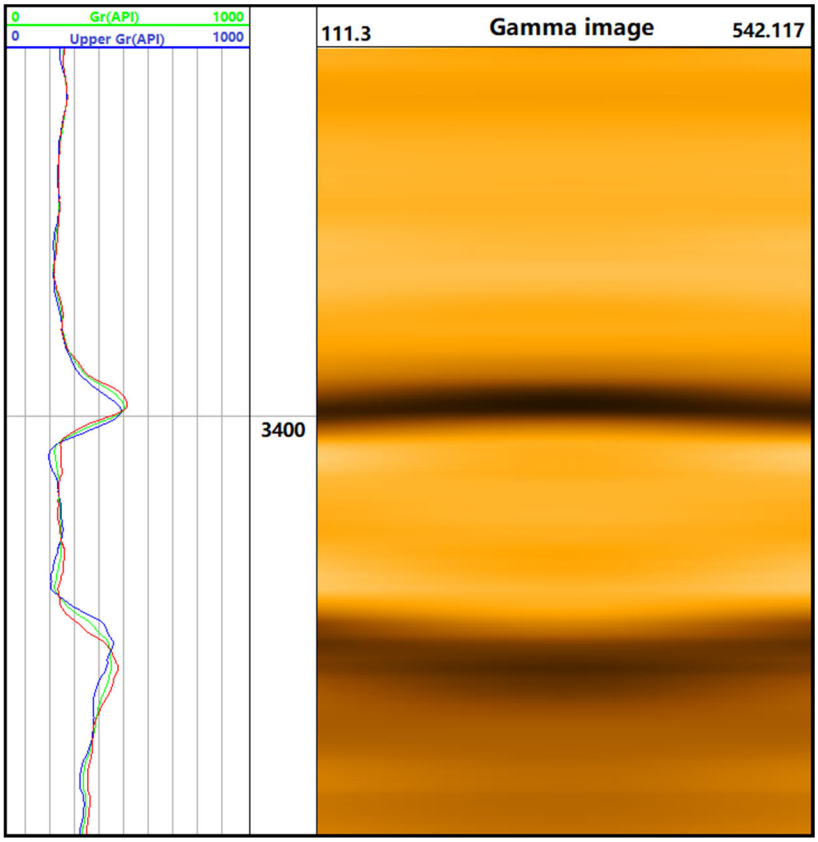

FIGURE 10. The gamma image of AA well.

as follows:

$$F_{n-1}(k) = \begin{cases} (1-\alpha)N_{n-1} & L_{n-1}(i) = R_{n-1}(i) \\ iN_{n-1} & L_{n-1}(i) \neq R_{n-1}(i) \end{cases} \quad (16)$$

where, $0 < \alpha < 1$, generally, $\alpha = 0.8$, N_{n-1} is expressed as follows:

$$N_{n-1} = \frac{\text{M-1}}{\text{n-1-}\alpha} \quad (17)$$

3) If $k < L_{n-1}(1)$, then $F_{n-1}(k) = 0$.

4) If $k \geq R_{n-1}(n-1)$, then $F_{n-1}(k) = \text{L-1}$.

Step 4: Calculate the distance between pixels, it is expressed as follows:

$$D_{n-1} = \frac{1}{N_{pix}(N_{pix}-1)} \sum_{i}^{M-2} \sum_{j=i+1}^{M-1} M_{n-1}(i) M_{n-1}(j)(j-i) \quad (18)$$

where, N_{pix} is the number of pixels, M is the number of gray levels.

Step 5: Repeat steps 2 to 4 if the groups is greater than 2.

Step 6: Find the maximum value of D_{i}, and its corresponding enhancement function is $F_{n-1}(k)$, then $F_{n-1}(k)$ is used to process the original image.

As shown in Figure 9(a), although the gamma image without noise removal and image enhancement can reflect the basic information such as lithology and interface of the formation, the boundary of geological change is not very obvious, which is not conducive to image interpretation. As shown in Figure 9(b), when the gamma image noise integrated with the quality control algorithm and image enhancement processing is well suppressed, the processing effect combines the advantages of the traditional enhancement algorithm. Not only the high contrast area is enhanced, but also the clarity of the low contrast area is significantly improved, more details are reflected, and the display effect is enhanced, which is more conducive to the interpretation and application of geosteering.

V. EXPERIMENT AND ANALYSIS

A. EXPERIMENT OF AA WELL

In this study, AA well in southwest is selected as the experimental well, which is a horizontal well. The target layer is thin and the formation dip angle is uncertain. In the actual construction process, the variation range of the vertical depth is relatively small, so it is more difficult to control the well trajectory in the horizontal section.

Based on the improved azimuth gamma imaging model established in this study, azimuth gamma data were collected in real time to verify the imaging effect of this model. As shown in Figure 10, when drilling to the depth about 3400m, the gamma value gradually increased,

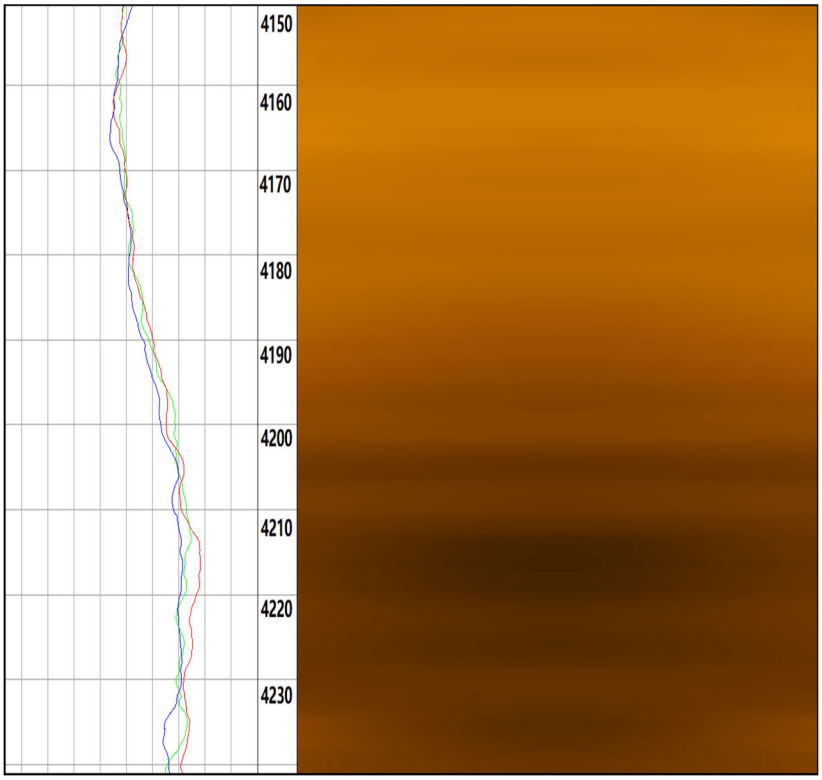

FIGURE 11. The gamma image of BB well.

the azimuth gamma detected the radioactivity intensity of the nearby formation as a high value, and the azimuth gamma image showed a concave arc, which shows the upper gamma senses the change in radioactive intensity more slowly than the other parts in the middle, indicating that the drilling trajectory is undercut and the borehole trajectory is out of the target horizon. Drilling was suspended immediately, and the observation of returned cuttings and gas logging analysis confirmed this judgment. The on-site engineer issued a command to increase the incline. When drilling to the depth of 3420m, gamma imaging showed that the borehole trajectory was upcut and the borehole trajectory returned to the target layer.

B. EXPERIMENT OF BB WELL

BB well is a well with high inclination. As shown in Figure 11, when drilling to the depth of 4192m, the gamma value gradually increase. The trajectory of azimuth gamma image is gradually cut down, and further drilling will gradually deviate from the target layer. The engineer increased the inclination according to the gamma image, then keeped the inclination for the continuing drilling.

Field experiments show that the model established in this paper can control the noise of downhole data to the greatest extent, and the data interpolation process compensates for the limitation of the limited number of azimuth gamma data collected in real time, which makes the gamma data have strong continuity. It is very important for the smooth transition of gamma images. In addition, the image enhancement technology makes the contrast and sharpness of the gamma image greatly improved. In short, the azimuth gamma imaging model established based on this study can generate high-quality gamma images, and the interface between reservoir and non-reservoir is clear, which improves the wellbore trajectory control ability and can help field engineers to better observe and make decisions.

VI. CONCLUSION

In this paper, an improved LWD azimuth gamma imaging model is studied in order to improve the traditional radio-gamma measurement technology. The HSI color space suitable for geological feature image display is selected in this model. Under this color space, the design of chromatographic and chromaticity calibration are completed. At the same time, this paper focuses on improving the gamma data sampling model, and a gamma data quality control algorithm is designed to filter the noise of the original data, which improves the quality of the original gamma data.

Furthermore, cubic spline interpolation is performed on the obtained original azimuth gamma data of different sectors, so that the model supports 360° gamma data at any angle and depth interval, which improves the excessive smoothness of the gamma image. In addition, this study also designed an image enhancement algorithm based on fast gray level grouping, which improved the contrast and sharpness of the

gamma image. In a word, the improved model improves the quality of azimuth gamma imaging from the original data and image processing, and the field experiment results are outstanding. It fully makes up for the lack of reference data, poor imaging quality and the difficulty of drilling tool callback, and truly realizes the rapid monitoring and analysis of drilling trajectory, which has high application value. The azimuth gamma image generated based on the model in this paper has high quality and can guide the geological guidance work well. However, if the edge contour of the gamma image can be recognized automatically, the result will be more intuitive, so we hope that the following work can focus on the edge detection method of the gamma image, which is meaningful.

REFERENCES

[1] G. Zhu, M. Gao, F. Kong, and K. Li, "Application of logging while drilling tool in formation boundary detection and geo-steering," *Sensors*, vol. 19, no. 12, p. 2754, Jun. 2019.
[2] C. Yuan, C. Zhou, F. Zhang, S. Hu, and C. Li, "A novel method for quantitative geosteering using azimuthal gamma-ray logging," *Appl. Radiat. Isot.*, vol. 96, pp. 63–70, Feb. 2015.
[3] K. Saikia, "A proposed methodology of 3D geomodeling-while-geosteering for optimum horizontal well placement and enhanced geological risk management," *Indian J. Mar. Sci.*, vol. 47, no. 4, pp. 826–830, Apr. 2018.
[4] L. I. U. Xiushan, "Directional deflection equations for steerable drilling tools and the control mechanism of wellbore trajectory," *Petroleum Explor. Develop.*, vol. 44, no. 5, pp. 788–793, Oct. 2017.
[5] H. Liang, J. Zou, Z. Li, M. J. Khan, and Y. Lu, "Dynamic evaluation of drilling leakage risk based on fuzzy theory and PSO-SVR algorithm," *Future Gener. Comput. Syst.*, vol. 95, pp. 454–466, Jun. 2019.
[6] C. Xiang, Z. Wang, and W. Kang, "Modeling and analysis of formation boundaries based on LWD natural gamma," *Oil Drilling Prod. Technol.*, vol. 35, no. 1, pp. 112–114, 2013.
[7] L. Xu, C. Huiszoon, J. Wang, B. Adolph, J. Yi, D. Cavin, G. Laughlin, E. Tollefsen, S. Jacobsen, and M. Boyce, "Spectral gamma-ray measurement while drilling," *Petrophys. Spwla J. Formation Eval. Reservoir Description*, vol. 57, no. 4, pp. 377–389, 2016.
[8] Z. Qin, H. Pan, Z. Wang, B. Wang, K. Huang, S. Liu, G. Li, A. A. Konaté, and S. Fang, "A fast forward algorithm for real-time geosteering of azimuthal gamma-ray logging," *Appl. Radiat. Isot.*, vol. 123, pp. 114–120, May 2017.
[9] I. R. Tribe, L. Burns, P. D. Howell, and R. Dickson, "Precise well placement with rotary steerable systems and logging-while-drilling measurements," *SPE Drilling Completion*, vol. 18, no. 1, pp. 42–49, Mar. 2003.
[10] H. Rohler, T. Bornemann, A. Darquin, and J. Rasmus, "The use of real-time and time-lapse logging-while-drilling images for geosteering and formation evaluation in the breitbrunn field, bavaria, germany," *SPE Drilling Completion*, vol. 19, no. 3, pp. 133–138, Sep. 2004.
[11] G. L. Moake, "Characterizing natural-gamma-ray tools without the API calibration formation," *Petrophysics*, vol. 58, no. 5, pp. 485–500, Oct. 2017.
[12] A. Suh, "Innovative instrumented motor with near-bit azimuthal gamma ray and inclination improves geosteering in thin-bedded formations," *Oil Gas Eur. Mag.*, vol. 39, no. 1, pp. 22–24, Mar. 2013.
[13] J. Yang, "Design of tubular azimuth gamma ray logging tool," *World J. Eng. Technol.*, vol. 4, no. 3, pp. 1–8, 2016.
[14] H. Liang, H. Chen, and Y. Lu, "Research on sensor error compensation of comprehensive logging unit based on machine learning," *J. Intell. Fuzzy Syst.*, vol. 37, no. 11, pp. 1–11, 2019.
[15] C. Ren, X. Hu, P. Qin, L. Li, and T. He, "Signal filtering for a small-diameter, dual-axis FOG inclinometer," *Sensor Rev.*, vol. 38, no. 3, pp. 353–359, Jun. 2018.
[16] M. Kamiyama and A. Taguchi, "HSI color space with same gamut of RGB color space," *IEICE Trans. Fundamentals Electron., Commun. Comput. Sci.*, vol. 100, no. 1, pp. 341–344, 2017.
[17] S. Ma, H. Ma, Y. Xu, S. Li, C. Lv, and M. Zhu, "A low-light sensor image enhancement algorithm based on HSI color model," *Sensors*, vol. 18, no. 10, p. 3583, Oct. 2018.
[18] G. Saravanan, G. Yamuna, and S. Nandhini, "Real time implementation of RGB to HSV/HSI/HSL and its reverse color space models," in *Proc. Int. Conf. Commun. Signal Process. (ICCSP)*, Apr. 2016, pp. 462–466.
[19] Q. Yu, K. Zhang, R. Zhou, C. Cui, F. Cheng, S. Fu, and R. Ye, "Calibration of a chromatic confocal microscope for measuring a colored specimen," *IEEE Photon. J.*, vol. 10, no. 6, pp. 1–9, Dec. 2018.
[20] H. He, J. Xiong, Y. Huang, and J. Xu, "Time-varying signal analysis method based on linear interpolation," in *Proc. ESMA*, Xian, China, 2019, Art. no. 032122.
[21] D. N. Varsamis and N. P. Karampetakis, "On the Newton bivariate polynomial interpolation with applications," *Multidimensional Syst. Signal Process.*, vol. 25, no. 1, pp. 179–209, Jan. 2014.
[22] Y. Zhao, Q. Fu, W. Lu, J. Yi, and H. Chu, "Wavelet denoising and cubic spline interpolation for observation data in groundwater pollution source identification problems," *Water Supply*, vol. 19, no. 5, pp. 1454–1462, Aug. 2019.
[23] M. C. Mariani and K. Basu, "Spline interpolation techniques applied to the study of geophysical data," *Phys. A, Stat. Mech. Appl.*, vol. 428, pp. 68–79, Jun. 2015.
[24] J. P. Boyd and L. F. Alfaro, "Hermite function interpolation on a finite uniform grid: Defeating the runge phenomenon and replacing radial basis functions," *Appl. Math. Lett.*, vol. 26, no. 10, pp. 995–997, Oct. 2013.
[25] Y. Yang, Z. Wei, A. Fourie, Y. Chen, B. Zheng, W. Wang, and S. Zhuang, "Particle shape analysis of tailings using digital image processing," *Environ. Sci. Pollut. Res.*, vol. 26, no. 25, pp. 26397–26403, Sep. 2019.
[26] D. S. Pandit, Y. V. N. Krishna Murthy, and V. Jayaraman, "Identification of sugarcane and onion crops using digital image processing of multidate, multisensor high-resolution satellite data," in *Proc. Agricult. Hydrol. Appl. Remote Sens.*, Dec. 2006.
[27] H. Liang and J. Zou, "Rock image segmentation of improved semi-supervised SVM-FCM algorithm based on chaos," *Circuits, Syst., Signal Process.*, vol. 39, no. 2, pp. 571–585, Feb. 2020.
[28] G. Raju and M. S. Nair, "A fast and efficient color image enhancement method based on fuzzy-logic and histogram," *AEU Int. J. Electron. Commun.*, vol. 68, no. 3, pp. 237–243, Mar. 2014.
[29] Y. C. Chang, C. M. Chang, L. C. Lai, and L. H. Chen, "Contrast enhancement and visual effects based on gray-level grouping," *J. Mar. Sci. Technol.*, vol. 22, no. 4, pp. 513–518, Aug. 2014.

HE ZHANG received the bachelor's degree in detection technology and automation instrumentation from Chongqing University, in 1995. He has served successively as the Director of the Laboratory, the Assistant to the Dean, and the Director of the Teaching and Research Department, Southwest Petroleum University. He has been engaged in the automatic detection technology, automatic control technology, and other fields of teaching and research work, focusing on intelligent instruments and intelligent systems and their applications.

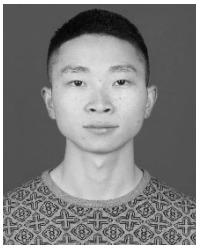

HONGQIANG LI was born in Sichuan, Mianyang, China, in 1994. He received the bachelor's degree in measurement and control technology and instruments from Southwest Petroleum University, in 2018, where he is currently pursuing the master's degree. Since 2018, he has been mainly engaged in drilling related data analysis and the research of drilling risk theory.

DENGYUN LU was born in 1965. He received the Ph.D. degree. He is currently a Professor-Level Senior Engineer with the China Petroleum and Natural Gas Group, Chuanqing Drilling Engineering Company Ltd., the Deputy Chief Division, and the Chuanqing Drilling Engineering Technology Research Institute Dean. He is mainly engaged in research, promotion, and management of new technologies in drilling and completion engineering.

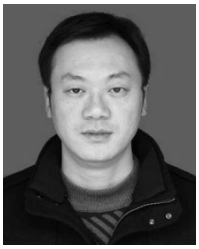

YI XIE was born in 1976. He received the degree in oil and gas well engineering from Southwest Petroleum University, in 2000. He is currently a Senior Engineer with the Chuanqing Drilling Engineering Technology Research Institute, China National Petroleum Corporation. He has published more than five articles. He is mainly engaged in the research and promotion of drilling and completion engineering.